

Nature of Spin Excitations in Two-Dimensional Mott Insulators: Undoped Cuprates and Other Materials

Chang-Ming Ho,^{1,*} V.N. Muthukumar,² Masao Ogata,³ and P.W. Anderson²

¹*Department of Applied Physics, University of Tokyo, 7-3-1 Hongo, Bunkyo-ku, Tokyo 113-8656, Japan*

²*Joseph Henry Laboratories of Physics, Princeton University, Princeton, New Jersey 08544*

³*Department of Physics, University of Tokyo, 7-3-1 Hongo, Bunkyo-ku, Tokyo 113-0033, Japan*

(Received 11 September 2000)

We investigate the excitation spectrum of a two-dimensional resonating valence bond (RVB) state. Treating the π -flux phase with antiferromagnetic correlations as a variational ground state, we recover the long wavelength magnon as an “RVB exciton.” However, this excitation does *not* exhaust the entire spectral weight and the high-energy spectrum is dominated by fermionic excitations. The latter can be observed directly by inelastic neutron scattering, and we predict their characteristic energy scales along different high symmetry directions in the magnetic Brillouin zone. We also interpret experimental results on two magnon Raman scattering and midinfrared absorption within this scenario.

DOI: 10.1103/PhysRevLett.86.1626

PACS numbers: 75.50.Ee, 75.40.Gb, 74.72.Dn

The undoped high T_c cuprates, such as La_2CuO_4 etc. [1], and compounds like $\text{Cu}(\text{DCO}_2)_2 \cdot 4\text{D}_2\text{O}$ (CFTD) [2,3] are ideal realizations of two-dimensional (2D) spin 1/2 Heisenberg antiferromagnets on the square lattice composed of Cu ions and, consequently, are interesting systems to study. The antiferromagnetism that is observed in the undoped cuprates plays a crucial role in some theories of the metallic state of doped Mott insulators. For these reasons, it is important to understand the nature of magnetic excitations in these materials. A direct way to probe the spectrum of magnetic excitations is inelastic neutron scattering (INS). The presence of long range antiferromagnetic order below the Néel temperature was established in the insulating cuprates by neutron scattering measurements [1]. Well-defined peaks, identified as magnons, have been observed to disperse along the magnetic zone boundary in different compounds [3,4]. Since then, a spin wave dispersion throughout the entire Brillouin zone in La_2CuO_4 has been extracted from INS measurements [5]. The antiferromagnetic correlation length diverges exponentially as the temperature is lowered, indicative of long range order at $T = 0$ [1,2]. This is in agreement with the analysis of the 2D antiferromagnetic Heisenberg model, with superexchange coupling J between adjacent spins, in terms of the quantum nonlinear σ model [6], and other approaches based on spin waves [7]. These results, concerning essentially the low-energy regime, are construed as evidence favoring the hypothesis that the excitation spectrum in these materials can be described adequately by renormalized spin wave theory [8].

On the other hand, optical probes such as Raman and midinfrared (IR) absorption spectroscopy highlight the inadequacy of the spin wave hypothesis. Typically, the positions of primary peaks observed in these experiments coincide reasonably well with calculations based on spin wave theory, but the observed line shapes cannot be explained, owing to the presence of finite spectral weight at high energies. For instance, the B_{1g} shift in Raman scat-

tering experiments spans a rather broad range of energies in insulating cuprates [9]. Recent measurements on insulating $\text{Sr}_2\text{CuO}_2\text{Cl}_2$ as well as in $\text{YBa}_2\text{Cu}_3\text{O}_{6.1}$ show very broad line shapes, spectral weight at higher energies, and a broad feature around $4J$ [10]. Optical absorption spectra show similar features. Experiments on insulating cuprates [11,12] show a primary peak identified with bimagnon plus phonon absorption [13]. But as in Raman scattering, the spectrum has a long tail extending to 8000 cm^{-1} in La_2CuO_4 and 6000 cm^{-1} in $\text{YBa}_2\text{Cu}_3\text{O}_6$. By analyzing the line shape and the high-energy spectra, Grüninger and co-workers have presented strong experimental evidence against the spin wave hypothesis for the insulating cuprates [12].

The two classes of experiments described in the preceding paragraphs do not necessarily contradict each other. Though the dispersing peaks observed in INS measurements can be interpreted as spin waves, an analysis of the *spectral weight* shows that long range order and spin waves can account for only about 50% of the observed spectrum [14]. These results indicate the presence of excitations beyond the one magnon mode. Thus, taken in conjunction, INS and optical spectroscopy suggest two possible theoretical approaches. One is to start from spin wave theory, and look for consistent explanations for the experimental results outlined above. This is not an easy task, as spin wave theory is an effective theory of long wavelength excitations. The other approach is to postulate a new set of excitations that offers a natural explanation of the high-energy spectra, and describing the magnons in terms of this new basis. It is the latter approach that we shall pursue.

In this paper, we consider the flux-phase resonating valence bond (RVB) theory, treated within the random phase approximation (RPA). Gapless spin wave excitations are recovered as a Goldstone mode. Besides this, the RVB theory also makes specific predictions about novel excitations—spin 1/2 flux fermions or spinons, and their direct

observation. We predict the characteristic energy scales of these excitations along various high symmetry directions and show how their presence can naturally account for the spectral weight seen at high energies in optical probes.

Our starting point is the π -flux state with staggered magnetization as a variational parameter [15]. For the case of the 2D Heisenberg antiferromagnet, the above state yields the best variational energy when the Gutzwiller constraint is enforced exactly [16]. We assume that the excited states of the flux fermion spectrum are also good variational states for the spin excitations of 2D Mott insulators. The π -flux state with staggered magnetization m is obtained in the mean-field approximation of the Hamiltonian

$$\mathcal{H} = -\frac{J_{\text{eff}}}{2} \sum_{\langle ij \rangle, \sigma} e^{i\Phi_{\square}} (f_{i\sigma}^{\dagger} f_{j\sigma} + \text{H.c.}) + V \sum_i n_{i\uparrow} n_{i\downarrow}, \quad (1)$$

which is an extension of the RVB mean-field theory [17]. The lattice fermions pick up a phase $\Phi_{\square} = \pi$ on hopping around an elementary plaquette, and also experience an on-site potential V , which is included to induce a spin density wave (SDW) coexisting with the flux order. The excitation spectrum is given by $E_{\mathbf{k}} = J_{\text{eff}} \sqrt{\cos^2 k_x + \cos^2 k_y + (m/2)^2}$ where m is determined self-consistently as $V^{-1} = N^{-1} \sum' E_{\mathbf{k}}^{-1}$, N being the number of lattice sites and the summation being over momenta in the magnetic Brillouin zone (MBZ).

The above Hamiltonian, with $J_{\text{eff}} \equiv J$, was first considered by Hsu [15]. Invoking a Gutzwiller approximation, Hsu determined the projected variational energy and the sublattice magnetization as a function of the SDW mass parameter m , induced by the potential V . The analysis of the excitation spectrum, however, is complicated by the Gutzwiller approximation. Owing to this difficulty, Hsu could only obtain the poles of the particle-hole Green's function ($S_z = \pm 1$ excitations) and not the complete dynamical spin susceptibility. To obtain the latter, we find it convenient to follow an equivalent approach, proposed first by Laughlin [18]. In this scheme, a spinon pair is created as a projected particle-hole excitation and the spinons constituting the pair experience an on-site repulsion, favoring the formation of an SDW. This interaction also enhances the exchange integral J to J_{eff} . The quantities J_{eff} and m are determined self-consistently to be $1.5J$ and 0.5 , respectively [18]. The Gutzwiller approximation technique employed by Hsu gives similar results.

We now obtain the dynamical spin susceptibility from Eq. (1) using RPA. The calculation parallels that of Schrieffer *et al.*, on the SDW instability of the 2D Hubbard model [19]. We obtain, for the (transverse) spin susceptibility, $S(\mathbf{q}, \omega) = -\text{Im} \chi^{+-}(\mathbf{q}, \omega)$, where

$$\chi^{+-}(\mathbf{q}, \omega) = \frac{\chi_0^{+-}(\mathbf{q}, \omega)}{1 - V \chi_0^{+-}(\mathbf{q}, \omega)} \quad (2)$$

$$\chi_0^{+-}(\mathbf{q}, \omega) = -\frac{1}{2N} \sum_{\mathbf{k}} \left[1 - \frac{\cos k_x \cos(k_x + q_x) + \cos k_y \cos(k_y + q_y) - (m/2)^2}{E_{\mathbf{k}} E_{\mathbf{k}+\mathbf{q}}} \right] \\ \times \left[\frac{1}{\omega - (E_{\mathbf{k}} + E_{\mathbf{k}+\mathbf{q}}) + i\delta} - \frac{1}{\omega + (E_{\mathbf{k}} + E_{\mathbf{k}+\mathbf{q}}) - i\delta} \right].$$

Here, χ_0^{+-} is defined as the time-ordered product $\langle TS^+ S^- \rangle$ with respect to the SDW ground state.

At the magnetic wave vector $\mathbf{q} = \mathbf{Q} = (\pi, \pi)$, $\chi(\mathbf{q}, \omega)$ is singular when $\omega = 0$. The spectrum is gapless, which result is guaranteed by the self-consistency of the RPA. Since the gapless mode is a bound state between particle-hole pairs, it is interpreted as an ‘‘RVB exciton’’. The dispersion of this mode can be obtained analytically. Evaluating $\lim_{\mathbf{q} \rightarrow \mathbf{Q}} \chi^{+-}$ for small ω , we obtain $\omega(\mathbf{q}) \approx 1.14 J_{\text{eff}} |\mathbf{q}|$. For arbitrary \mathbf{q} , Eq. (2) has to be evaluated numerically. The results for $S(\mathbf{q}, \omega)$ are shown in Fig. 1. For each \mathbf{q} , we see a strong peak at low energy. This magnon (or RVB exciton) peak disperses as \mathbf{q} varies. By tracking the position of the intense peaks at low energy, we obtain the magnon dispersion for the entire MBZ (see Fig. 2), recovering Hsu's results [15]. Near the zone boundary, the dispersion deviates from that of linear spin waves.

It is important to realize that our approach is much more than just a complicated way of describing magnons. This is borne out by our explicit evaluation of $S(\mathbf{q}, \omega)$. For example, consider $S(\mathbf{q}, \omega)$, at (π, π) in Fig. 1. The intensity drops at higher energy, and grows again at

$\omega \approx 0.5 J_{\text{eff}}$. The intensity at higher energies is interpreted as the manifestation of the particle-hole (spinon) excitations. Within this interpretation, we can estimate the characteristic energy at which the continuum becomes visible. Consider a spin-flip excitation with momentum \mathbf{q} as a convolution of particle-hole excitations. Then, its energy $\omega(\mathbf{q})$ is given by $\omega(\mathbf{q}) = E_{\mathbf{q}-\mathbf{k}} + E_{\mathbf{k}}$, where we have ignored the residual interaction. For $\mathbf{q} = \mathbf{Q}$, $\omega(\mathbf{Q}) = 2J_{\text{eff}} \sqrt{\cos^2 k_x^2 + \cos^2 k_y^2 + (m/2)^2}$. Its minimum, occurring when the two fermions are created at the Dirac point $(\pi/2, \pi/2)$, is exactly mJ_{eff} , as seen in Fig. 1. This analysis shows that the continuum emerging for energies $0.5J_{\text{eff}}$ and above can be interpreted as arising from a convolution of free flux fermions or spinons. The line shape is, however, determined by the interaction. Because of the phase space available for convolution, the onset of the continuum is a strong function of momentum. Hence, as seen in Fig. 1, the magnon peak as well as the lower boundary of the flux-fermion continuum shift in energy, as \mathbf{q} is varied. As $\mathbf{q} \rightarrow (\pi, 0)$, the onset of the continuum shifts towards lower energies. At $(\pi, 0)$, there is no easy way to isolate the magnon and spinon

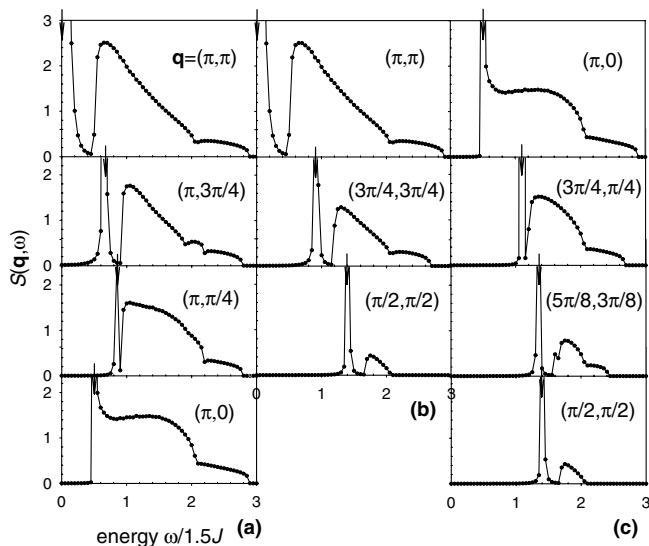


FIG. 1. Spin susceptibility $S(\mathbf{q}, \omega)$ as a function of energy ω for various \mathbf{q} 's in the direction of (a) (π, π) to $(\pi, 0)$, (b) (π, π) to $(\pi/2, \pi/2)$, and (c) $(\pi, 0)$ to $(\pi/2, \pi/2)$ along the zone boundary. The results are obtained using Eq. (2) with $\delta = 0.001$ and 3000 \mathbf{q} points in the MBZ. The energy is in units of $1.5J$. The small vertical arrows mark the positions of the magnon peaks.

contributions [20]. In Fig. 1(b), we display the behavior of $S(\mathbf{q}, \omega)$ along the direction $(\pi, \pi) \rightarrow (\pi/2, \pi/2)$. In this case, the lower boundary of the fermion continuum shifts towards *higher* energies. At $(\pi/2, \pi/2)$, we find the onset of the continuum around $1.7J_{\text{eff}}$. As before, this value can be understood by considering the spin-flip excitation with momentum $(\pi/2, \pi/2)$ as a particle-hole

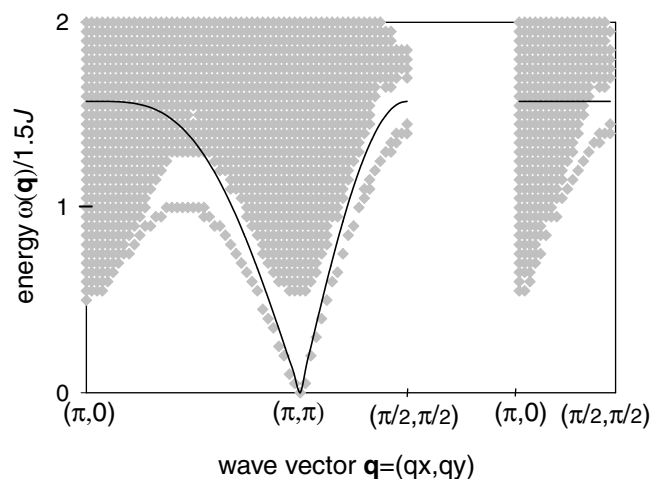


FIG. 2. Spectrum along high symmetry directions in the MBZ deduced from spin susceptibility intensities $S(\mathbf{q}, \omega)$. Each (gray) diamond marks the $S(\mathbf{q}, \omega)$ which has intensity larger than 1.5 (arbitrary unit), as chosen here. The low-energy branch represents the magnon dispersion. The broad shaded region corresponds to the spinon continuum. The solid line represents the spin-wave dispersion, $2Z_c J \sqrt{1 - [(\cos k_x + \cos k_y)/2]^2}$ with $Z_c \sim 1.18$ the renormalization factor.

pair. A similar analysis as in the previous case yields a minimum energy, $J_{\text{eff}}[m + 2\sqrt{2 + (m/2)^2}]/2$ at the Dirac point $(\pi/2, \pi/2)$. For $m = 0.5$, this turns out to be $1.7J_{\text{eff}}$, confirming our interpretation.

From our results for the magnon peak and the fermion continuum, we obtain the spectrum of excitations over the whole MBZ, which is shown in Fig. 2. Note that by putting $\Phi_{\square} = 0$ in Eq. (1), results from the weak coupling approach to the Heisenberg antiferromagnet [19] can be obtained. We have verified that the excitation spectrum, in this case, is distinct from ours [20]. Thus, our calculations are specific to the existence of a π -flux phase [20]. Our results for small $\mathbf{q} \approx \mathbf{Q}$ are consistent with calculations based on the bosonic RVB scheme [21]. At higher energies, it has been shown [22] that the bosonic RVB state can support vortexlike topological excitations that are fermionic. This agrees with our picture of fermionic excitations at high energies. The shaded region in Fig. 2 depicts these excitations and can, in principle, be observed directly by INS. At the magnetic wave vector \mathbf{Q} , there is a well-defined gap between the strong magnon peak and the spinon continuum, which may facilitate detection of the continuum along this direction. For typical values of the superexchange coupling J in undoped cuprates, this gap is of the order of 100 meV. Recently, Coldea *et al.* [5] have reported results from high-energy (0.1–0.5 eV) neutron scattering in La_2CuO_4 . Given the possibility of studying high-energy spin excitations with enhanced resolution, INS may be a good probe for the direct observation of spinon excitations, should they exist. It is therefore extremely interesting to examine, both theoretically and experimentally, whether our predictions are realized in this measurement. Experiments show that as \mathbf{q} varies from $(\pi, 0)$ to $(\pi/2, \pi/2)$, the spectral weight at high energies decreases. This is certainly consistent with our calculation. A detailed comparison incorporating appropriate structure factors for neutron scattering is forthcoming [20].

Let us now turn our attention to the two magnon experiments. As mentioned earlier, these experiments are characterized by a broad spectral distribution of intensity and secondary peaks. Both these features can be explained naturally within our scheme. First, let us consider the observed widths of the primary peaks in two magnon Raman scattering. We identify two reasons why the observed linewidths are very broad. (a) Conventional spin wave theory yields magnons that do not disperse along the zone boundary, leading to a singularity in the density of magnon states. Consequently, the Raman spectrum is dominated by zone boundary magnons. The singularity is, however, smoothed by magnon-magnon interactions. On the other hand, in the RVB scenario, a broad spectrum is obtained even with noninteracting magnons. This is because the low lying mode in Fig. 2 disperses along the zone boundary and there is no singularity in the density of states. Thus, the two magnon spectrum is *not* dominated by zone boundary excitations, and is broader than the spectrum obtained from linear spin wave theory. (b) In addition to this

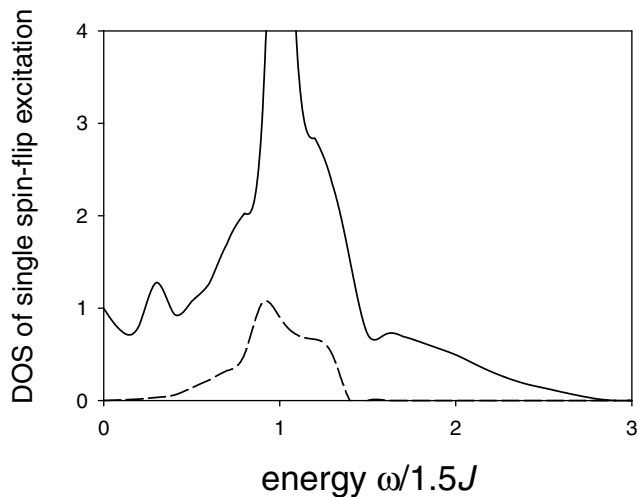


FIG. 3. Density of states of a single spin-flip excitation. The dashed line is obtained when only the magnon peak is considered. The solid line is $\pi^{-1} \sum_{\mathbf{q}} S(\mathbf{q}, \omega)$.

intrinsic width of the two magnon spectrum, we expect the line shape to be broadened further by the contribution from the spinon continuum as is evident from Fig. 2. To illustrate the above, we calculate the density of states (DOS) corresponding to *one* spin-flip excitation $\sum' \delta[\omega - \omega(\mathbf{q})]$. In Fig. 3, the dashed line shows the DOS obtained by considering only the magnon peak. To incorporate the entire excitation spectrum, i.e., both the magnon and the spinon excitations, we also plot (solid line) $\pi^{-1} \sum_{\mathbf{q}} S(\mathbf{q}, \omega)$. As seen in the figure, the presence of spinon excitations leads to a hump at $\omega \sim 2J$, followed by a long tail extending to energies $\omega \sim 4J$ and beyond. These features are clearly absent when only the magnon peak is considered. The results indicate that the two magnon DOS (relevant to Raman experiments) would show a primary peak around $\omega \sim 3J$ (from the low lying mode) and a broad hump at $\omega \sim 4J$ (arising from the continuum). We expect similar features in the midinfrared absorption spectra. In this case, the spectrum is broader as the two spin-flip excitation can carry finite momentum, and the final result involves summing over all such momenta. To summarize this discussion, the unconventional dispersion of the magnon in the RVB scheme leads to broad primary peaks in the optical spectra and the contribution of the spinon continuum leads to secondary peaks.

In conclusion, the observation of dispersing magnon peaks in spin 1/2 Mott insulators does not rule out the existence of spinons *per se*. The magnon can be recovered as an RVB exciton and the presence of spinons can be directly observed by a careful analysis of the line shapes obtained from inelastic neutron scattering. We have obtained, within the framework presented in this paper, the characteristic energy scales at which the spinon continuum can be observed. Dispersing magnons seen in neutron scatter-

ing and the observation of spectral weight at high energies in optical experiments, as well as the ubiquitous secondary peaks, can all be reconciled by our picture. While our results do not prove the existence of spinons, they certainly demonstrate how their presence modifies the spin excitation spectrum. It is hoped that these results would spur further experimental investigation of these issues, in particular, a careful analysis of the high-energy spin excitation spectrum.

We thank G. Aeppli, B. Keimer, P. A. Lee, T. K. Lee, N. Nagaosa, T.-K. Ng, and Z. Y. Weng for discussions. C.M.H. was supported in Japan by the Grant-In-Aid for the COE project from Manbusho. Work at Princeton is supported by NSF Grant No. DMR-9104873.

*Present address: Physics Division, National Center for Theoretical Sciences, P.O. Box 2-131, Hsinchu, Taiwan 300.

- [1] See, for example, M. A. Kastner *et al.*, Rev. Mod. Phys. **70**, 897 (1998), and references therein.
- [2] S. J. Clarke *et al.*, J. Phys. Condens. Matter **4**, L71 (1992); H. M. Rønnow, D. F. McMorrow, and A. Harrison, Phys. Rev. Lett. **82**, 3152 (1999).
- [3] S. J. Clarke *et al.*, Solid State Commun. **112**, 561 (1999).
- [4] S. M. Hayden *et al.*, Phys. Rev. Lett. **67**, 3622 (1991).
- [5] R. Coldea *et al.*, Physica (Amsterdam) **276B-278B**, 592 (2000); R. Coldea *et al.*, cond-mat/0006384; G. Aeppli (private communication).
- [6] S. Chakravarty, B. I. Halperin, and D. R. Nelson, Phys. Rev. B **39**, 2344 (1989).
- [7] A. Cuccoli *et al.*, Phys. Rev. Lett. **77**, 3439 (1996).
- [8] E. Manousakis, Rev. Mod. Phys. **63**, 1 (1991).
- [9] See, for example, S. Sugai *et al.*, Phys. Rev. B **42**, 1045 (1990).
- [10] G. Blumberg *et al.*, Phys. Rev. B **53**, R11 930 (1996).
- [11] J. D. Perkins *et al.*, Phys. Rev. Lett. **71**, 1621 (1993); Phys. Rev. B **58**, 9390 (1998).
- [12] M. Grüninger, Ph.D. thesis, University of Groningen, 1999; M. Grüninger *et al.*, Phys. Rev. B **62**, 12 422 (2000).
- [13] J. Lorenzana and G. A. Sawatzky, Phys. Rev. Lett. **74**, 1867 (1995); Phys. Rev. B **52**, 9576 (1995).
- [14] See, for example, P. Bourges *et al.*, Phys. Rev. Lett. **79**, 4906 (1997); R. R. P. Singh and M. P. Gelfand, Phys. Rev. B **52**, R15 695 (1995); G. Aeppli *et al.*, Phys. Status Solidi (b) **215**, 519 (1999).
- [15] T. C. Hsu, Phys. Rev. B **41**, 11 379 (1990).
- [16] A. Hameda and M. Ogata, Phys. Rev. B **60**, R9935 (1999).
- [17] G. Kotliar, Phys. Rev. B **37**, 3664 (1988); I. Affleck and J. B. Marston, *ibid.* **37**, 3774 (1988).
- [18] R. B. Laughlin, J. Low Temp. Phys. **99**, 443 (1995).
- [19] J. R. Schrieffer, X. G. Wen, and S. C. Zhang, Phys. Rev. B **39**, 11 663 (1989).
- [20] We refer to a forthcoming paper for details.
- [21] A. Auerbach and D. P. Arovas, Phys. Rev. Lett. **61**, 617 (1988); D. Yoshioka, J. Phys. Soc. Jpn. **58**, 32 (1989); Sanjoy Sarker *et al.*, Phys. Rev. B **40**, 5028 (1989).
- [22] Tai-Kai Ng, Phys. Rev. B **52**, 9491 (1995).